

Journal Article

**Preparation and emulsifying properties of trace elements fortified gum arabic**

Hu, B., Han, L., Kong, H., Nishinari, K., Phillips, G.O., Yang, J., Fang, Y.

This article is published by Elsevier. The definitive version of this article is available at:  
<https://www.sciencedirect.com/science/article/pii/S0268005X18310804#!>

---

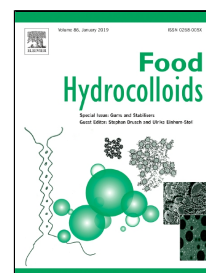
**Recommended citation:**

Hu, B., Han, L., Kong, H., Nishinari, K., Phillips, G.O., Yang, J., Fang, Y. (2018) 'Preparation and emulsifying properties of trace elements fortified gum arabic', *Food Hydrocolloids*, vol 88, pp. 43-49. doi: 10.1016/j.foodhyd.2018.09.027

# Accepted Manuscript

Preparation and emulsifying properties of trace elements fortified gum arabic

Bing Hu, Lingyu Han, Huiling Kong, Katsuyoshi Nishinari, Glyn O. Phillips, Jixin Yang, Yapeng Fang



PII: S0268-005X(18)31080-4

DOI: 10.1016/j.foodhyd.2018.09.027

Reference: FOOHYD 4665

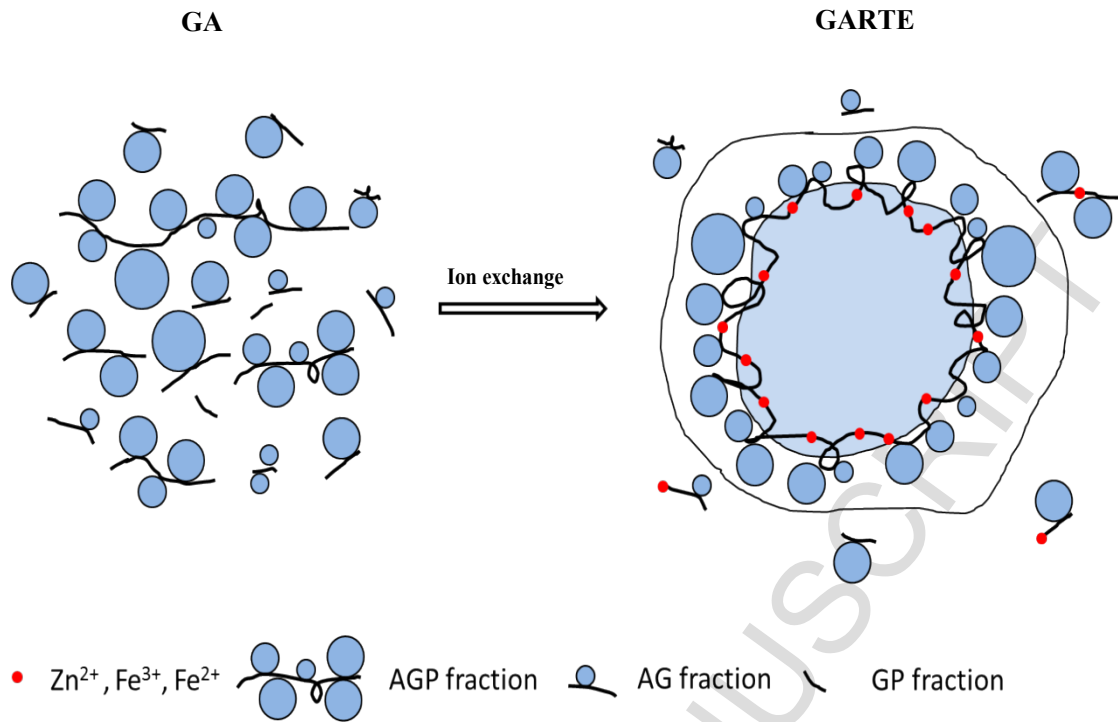
To appear in: *Food Hydrocolloids*

Received Date: 13 June 2018

Accepted Date: 19 September 2018

Please cite this article as: Bing Hu, Lingyu Han, Huiling Kong, Katsuyoshi Nishinari, Glyn O. Phillips, Jixin Yang, Yapeng Fang, Preparation and emulsifying properties of trace elements fortified gum arabic, *Food Hydrocolloids* (2018), doi: 10.1016/j.foodhyd.2018.09.027

This is a PDF file of an unedited manuscript that has been accepted for publication. As a service to our customers we are providing this early version of the manuscript. The manuscript will undergo copyediting, typesetting, and review of the resulting proof before it is published in its final form. Please note that during the production process errors may be discovered which could affect the content, and all legal disclaimers that apply to the journal pertain.



1           **Preparation and emulsifying properties of trace elements fortified gum arabic**

2

3   Bing Hu<sup>a, b</sup>, Lingyu Han<sup>a, b</sup>, Huiling Kong<sup>a, b</sup>, Katsuyoshi Nishinari<sup>a, b</sup>, Glyn O. Phillips<sup>a, b</sup>, Jixin  
4   Yang<sup>c</sup> and Yapeng Fang<sup>a, b, d\*</sup>

5

6   <sup>a</sup> Hubei International Scientific and Technological Cooperation Base of Food Hydrocolloids,  
7   Hubei University of Technology, Wuhan 430068, China;

8   <sup>b</sup> Glyn O. Phillips Hydrocolloid Research Centre at HUT, School of Food and Biological  
9   Engineering, Hubei University of Technology, Wuhan 430068, China;

10   <sup>c</sup> School of Applied Science, Computing and Engineering, Wrexham Glyndwr University, Plas  
11   Coch, Mold Road, Wrexham LL11 2AW, United Kingdom;

12   <sup>d</sup> Department of Food Science and Engineering, School of Agriculture and Biology, Shanghai Jiao  
13   Tong University, Shanghai 200240, China

14

15

16   \*Correspondence Author: Prof. Yapeng Fang, Glyn O. Phillips Hydrocolloid Research Centre at  
17   HUT, School of Food and Biological Engineering, Hubei University of Technology, Wuhan  
18   430068, China. Email: [fangypphrc@163.com](mailto:fangypphrc@163.com); Tel: 86-(0)-27-59750470.

19

20

21

22

23

24

25   **Key words:** Gum arabic, trace elements, emulsion.

26

27

28

29

30 **Abstract**

31 Gum arabic was enriched with trace elements ( $Zn^{2+}$ ,  $Fe^{3+}$ ,  $Fe^{2+}$ ) by ion exchange against  
32  $ZnCl_2$ ,  $FeCl_3$  and  $FeCl_2$ . Trace elements content, molecular parameters and emulsifying properties  
33 of the gum arabic rich in trace elements (GARTE) were characterized by flame atomic absorption  
34 spectrometry (FAAS), gel permeation chromatography-multi angle laser light scattering (GPC-  
35 MALLS), interfacial rheometer, laser particle analyzer and zeta potentiometry. With trace  
36 elements, molecular weight and arabinogalactan protein (AGP) content of gum arabic have  
37 increased **probably** due to the high surface energy leading to the aggregation of protein. GARTE  
38 has good emulsion stability performance with increasing molecular weight and AGP content  
39 compared to the control gum arabic. GARTE can be applied as a natural functional ingredient for  
40 trace element fortification, where the ferric ions and zinc ions are chelated by the self-assembled  
41 polymer host.

42

43

44

45

46

47

48

49

50

51

52

53

54

55

56

57

58

59

60

61

62

63

64

65

66

67

## 68 1. Introduction

69 Trace elements have been classified as trace minerals (<100 mg/day intake) which are needed in  
70 small quantities and used by all living organisms. They are imperative for optimum host response.  
71 Amidst the array of micronutrients, trace elements make up about 4% of the body weight and are  
72 mainly present in the skeleton, enzymes and hormones. They help in regulating and maintaining  
73 the normal heart rhythm, muscle contraction, nerve conduction and the acid–base balance  
74 (Schifferle, 2010). Populations worldwide are prone to their insufficiency owing to lifestyle  
75 changes or poor nutritional intake. A growing list of trace element utilization pathways highlights  
76 the importance of these elements for life (Prentice, 2005; Swinburn & Ravussin, 1994). Zinc (Zn)  
77 is thought to be essential for all organisms and suggested to be a key element in the origin of life  
78 (Mulikdjanian, 2009). Zn is an integral component of a large number of macromolecules, where it  
79 can maintain the stability of the cell membrane and activate more than 200 kinds of enzymes, get  
80 involved in nucleic acid and energy metabolism, and promote sexual, anti-bacterial, anti-  
81 inflammatory functions (Dupont, *et al.*, 2010; Dupont, *et al.*, 2006; Gaither & Eide, 2001; Hantke,  
82 2005; Murakami & Hirano, 2008; Prasad, 1995). Zn deficiency is more prevalent in children,  
83 elderly and patients with immunosuppressive disorders due to dietary deficiencies or poor  
84 absorption (Dawson, *et al.*, 2013). Its deficiency leads to the increase of frequency for infections  
85 and degenerative pathologies (Dawson, *et al.*, 2013; Meunier, *et al.*, 2005). Iron (Fe) compounds  
86 are ubiquitous in industrial applications, have vital functions in biological processes, and are  
87 essential in the human diet. They are crucial for erythropoiesis and haemoglobin and play an  
88 important role of oxygen transport in the blood (Schifferle, 2010). Fe is the active ingredient of  
89 many enzymes, metabolism and redox reactants (Hou, *et al.*, 2014; Listed, 1968; Matzner, *et al.*,  
90 1979; Trumbo, *et al.*, 2001). If the human body lacks sufficient intake, iron deficiency and anemia  
91 develop, which are prevailing global health issues (Chakraborty, *et al.*, 2014; Mukhopadhyay &  
92 Mohanaruban, 2002; Touitou, *et al.*, 1985).

93 Gum arabic (GA) is one of the popular ingredients widely used in the food and pharmaceutical  
94 industries (Guan & Zhong, 2014). It is a branched-chain, complex polysaccharide, either neutral  
95 or slightly acidic, found as mixed calcium, magnesium and potassium salts of polysaccharidic  
96 acids (Ali, Ziada, & Blunden, 2009). Three different fractions could be separated from gum

97 arabic, namely, arabinogalactan (AG, ~90% of total mass), arabinogalactan protein (AGP, ~10%  
98 of total mass) and glycoprotein (GP, ~1% of total mass) (Randall, Phillips, & Williams, 1989).  
99 GA is commonly used as an emulsifier to stabilize emulsions, the emulsifying property of which is  
100 provided by an excellent interfacial property of AGP. The structure of AGP is represented by a  
101 ‘wattle blossom-model’, which has, upon suggestion, provided both hydrophobic polypeptide  
102 chain and hydrophilic carbohydrate blocks, conferring good emulsification characteristics  
103 (Castellani, Guibert, *et al.*, 2010; Gomes, *et al.*, 2010; Jayme, Dunstan, & Gee, 1999; Mahendran,  
104 *et al.*, 2008). The stabilizing function of GA is provided by repulsive electrostatic and steric  
105 interactions after the polypeptide moieties adsorb on to the oil droplet surface and the  
106 polysaccharide chains protrude in the aqueous phase (Dickinson, 2003). The high water solubility  
107 and low solution viscosity are two additional features making GA a popular ingredient (Gomes, *et*  
108 *al.*, 2010).

109 Balanced levels of trace minerals like zinc (Zn) and iron (Fe) are essential to prevent  
110 progression of chronic conditions (Zhang & Gladyshev, 2011). To overcome this problem, zinc  
111 and iron supplementation and food fortification strategies are being actively pursued (Allen, *et al.*,  
112 2006; Hilty, *et al.*, 2010). The application of gum arabic as food-grade functional polymer hosts  
113 for complexation of trace elements into supramolecular structures could be an alternative strategy  
114 of immediate practical significance. Herein, we have developed a method to transform commercial  
115 gum arabic into the zinc and iron carrier by ion exchange against  $ZnCl_2$ ,  $FeCl_2$  and  $FeCl_3$ . Flame  
116 atomic absorption spectrophotometry (FAAS) confirms the transformation to GARTE, whereas all  
117 other ionic species remain at very low concentrations. The emulsifying performance of the  
118 GARTE (GA/ $Zn^{2+}$ , GA/ $Fe^{3+}$ , GA/ $Fe^{2+}$ ) was investigated as well. The purpose of this study is to  
119 gain a natural functional polysaccharide containing essential trace elements, and investigate the  
120 impact of ionic binding on the emulsifying properties of GA.

121

## 122 2. Materials and methods

### 123 2.1 Materials

124 Gum arabic (GA) was provided by San-Ei Gen F.F.I. Inc. (Osaka, Japan) in a spray dried  
125 powder. GA contains 5.56% moisture. Zinc chloride ( $\text{ZnCl}_2$ ), anhydrous ferric chloride ( $\text{FeCl}_3$ ),  
126 iron dichloride tetrahydrate ( $\text{FeCl}_2 \cdot 4\text{H}_2\text{O}$ ) were purchased from Chinese Medicine Group  
127 Chemical Reagent Co. Ltd. (Shanghai, China). Medium-chain triglyceride (MCT) was purchased  
128 from KLK OLEO Ltd., Malaysia. Hydrogen ion exchange resin was purchased from Sigma-  
129 Aldrich Trading Co. Ltd., USA. Doubly-distilled deionized water was used in all the experiments.

### 130 2.2 Preparation and characterization of GARTE

131 GARTE ( $\text{GA}/\text{Zn}^{2+}$ ,  $\text{GA}/\text{Fe}^{3+}$ , or  $\text{GA}/\text{Fe}^{2+}$ ) was prepared by ion exchange method. To prepare  
132  $\text{GA}/\text{Zn}^{2+}$  as an example: hydrogen ion exchange resin was treated with 1 M HCl (400 ml) for 4 h  
133 and washed extensively with deionized water to remove free hydrogen ions. 0.5 M  $\text{ZnCl}_2$  (800 ml)  
134 was added to the resin for 4 h, followed by deionized water rinse. 0.5 M  $\text{AgNO}_3$  solution was used  
135 to confirm if free  $\text{Cl}^-$  ions in the resin were removed completely. 15% GA (200 g) solution was  
136 added to the resin for 4 h to allow  $\text{Zn}^{2+}$  exchange onto GA, followed by freeze drying. The same  
137 method was used to prepare  $\text{GA}/\text{Fe}^{3+}$  and  $\text{GA}/\text{Fe}^{2+}$  with  $\text{FeCl}_3$  and  $\text{FeCl}_2 \cdot 4\text{H}_2\text{O}$ , respectively.

138 The control GA and GARTE samples were characterized by gel permeation chromatography  
139 coupled with multi-angle light scattering (GPC-MALLS). The GPC-MALLS system consisted of  
140 a Waters 515 HPLC pump (Waters Co., Massachusetts, USA), a Superose 6 10/300GL column  
141 (GE Healthcare, USA), a UV detector at 214 nm (Shimadzu Technologies, Kyoto, Japan), a  
142 DAWN HELEOS light scattering detector (Wyatt Technology Co., CA, USA) with a solid-state  
143 laser operating at 658 nm, and a refractive index detector (Optilab rEX, Wyatt Technology Co.,  
144 CA, USA). 0.2 M NaCl solution was used as an eluent and delivered at a constant flow rate of 0.4  
145 ml/min. 200  $\mu\text{l}$  of 2 mg/ml GA solution (in 0.2 M NaCl) was injected for analysis after filtration  
146 through 0.45  $\mu\text{m}$  filter. A refractive index increment  $\text{dn}/\text{dc}$  value of 0.145 was used for molecular  
147 parameter analysis of GA and GARTE. The data were analyzed with ASTRA software Version  
148 5.3.4.14.



## 149 2.3 Elemental analysis

150 The element content analysis of GA and GARTE was carried out by atomic absorption  
151 spectrometry equipped with a Zeeman background corrector (GBC Avanta M, Australia). An  
152 atomizer with an air/acetylene burner in voltage under  $220\pm 10V$  was used for determining all the  
153 elements investigated. The operating conditions were those recommended by the manufacturer,  
154 unless specified otherwise. The acetylene flow rate and the burner height were adjusted in order to  
155 obtain the maximum absorbance signal, while aspirating the analyte solution in methanol  
156 containing 0.1 M nitric acid. For discrete volume sampling, a volume of 100  $\mu\text{L}$  of the final  
157 solution was introduced into the nebulizer of the spectrometer by a manual sample injector that  
158 was connected to the nebulizer by the sample aspiration tubing. Absorbance signals as peak height  
159 were measured (Chen & Teo, 2001; Tokalioğlu, Kartal, & Elçi, 2000). High purity reagents and  
160 doubly-distilled deionized water were used for all the analyses. Standard stock solutions  
161 containing 1000  $\mu\text{g/mL}$  were prepared from sulfate of  $\text{Zn}^{2+}$ ,  $\text{Fe}^{2+}$  in 1 M of  $\text{HNO}_3$ .

## 162 2.4 Interfacial adsorption and emulsion properties of GARTE

### 163 2.4.1 Interfacial tension measurements

164 The interfacial adsorption of GA and GARTE at the oil-water interface changing with time was  
165 measured by a drop profile tensiometer (Teclis Tracker, France). The experiments were carried  
166 out at  $25 \pm 1^\circ\text{C}$ . A pendant drop of GA or GARTE solution was formed at the tip of the needle of  
167 a syringe whose verticality could be controlled. The needle was submerged in an optical glass  
168 cuvette containing MCT, which was located between a light source and a high-speed charge  
169 couple device (CCD) camera. The drop profile was recorded by the CCD camera and analyzed  
170 according to the Laplace equation (Castellani, Gaillard, *et al.*, 2010; Castellani, Guibert, *et al.*,  
171 2010; Oscar, *et al.*, 2010).

### 172 2.4.2 GARTE emulsion preparation

173 Each 5%(w/w) GA or GARTE ( $\text{GA/Zn}^{2+}$ ,  $\text{GA/Fe}^{3+}$ ,  $\text{GA/Fe}^{2+}$ ) solution was put on a roller mixer  
174 at  $25\pm 1^\circ\text{C}$  overnight. MCT was added to the gum solutions to achieve a final concentration of  
175 5%(w/w) in the emulsions. The systems were pre-homogenized for 3 min at 26,000 rpm using a

176 high-speed blender (Polytron PT 2100, Switzerland). The primary emulsions were further  
177 homogenized with a high-pressure homogenizer (Microfluidic M-110L, USA) at 75 MPa for one  
178 pass. The homogenization was carried out in an ice bath to minimize the extent of lipid oxidation.

#### 179 2.4.3 Droplet size distribution measurements

180 The droplet size distribution of the GARTE emulsions at 60°C was determined to evaluate the  
181 properties and stability using a laser diffraction technique (Master-Sizer 2000, Malvern  
182 Instruments Ltd.). The emulsions were diluted to achieve a laser obscuration slightly above 10%  
183 and stirred continuously to avoid multiple scattering effects. The refractive index of sample was  
184 1.52 with an absorption coefficient of 0.01. The particle size is given as the volume-weighted  
185 mean diameter ( $D[4, 3]$ ),  $D[4, 3] = (\sum n_i d_i^4 / \sum n_i d_i^3)$ , where  $n_i$  is the number of droplets with diameter  
186  $d_i$ .  $D_{4,3}$  was reported as the average of triplicates.

#### 187 2.4.4 Zeta potential measurements

188 Zeta potential  $\zeta$  of emulsion was measured on a Zetasizer Nano-ZS apparatus (Malvern  
189 Instruments, U.K.) equipped with an MPT-2 pH autotitrator (4mW He/Ne laser emitting at 633  
190 nm). Electrophoretic mobility  $U_E$  of charged particles was measured by means of laser Doppler  
191 velocimetry (LDV), and  $\zeta$  was calculated according to the Henry equation: (Li, *et al.*, 2012)

$$192 \quad U_E = \frac{2\varepsilon\zeta f(Ka)}{3\eta} \quad (1)$$

193 where  $\varepsilon$  is the dielectric constant,  $\eta$  is the viscosity of medium, and  $f(Ka)$  is the Henry function  
194 which possesses a value of 1.5 under the Smoluchowski approximation.

195

### 196 3. Results and discussion

#### 197 3.1 Trace element content and molecular parameters of GARTE

198 Trace element contents of GA, GA/Zn<sup>2+</sup>, GA/Fe<sup>3+</sup>, GA/Fe<sup>2+</sup> samples were shown in Table 1.  
199 The trace element contents of control GA sample (without ion exchange) from high to low are: K>  
200 Na> Ca> Mg> Zn> Fe> Cu. The content of corresponding target elements (Zn<sup>2+</sup>, Fe<sup>3+</sup>, Fe<sup>2+</sup>) in  
201 GARTEs have significantly increased with other elements (K, Na, Ca, Mg) decreasing after ion  
202 exchange. The contents of Zn<sup>2+</sup>, Fe<sup>3+</sup> and Fe<sup>2+</sup> in GARTEs increase respectively by 27, 162 and  
203 1097 times, compared to control GA. The enrichment of Fe<sup>2+</sup> by ion exchange method is the most  
204 efficient. It clearly reveals that the GARTE can be successfully prepared by ion exchange method.  
205 The molecular parameters of control GA and GARTEs are shown in Table 2. The molecular  
206 weights and AGP contents of GARTEs have increased after ion exchange, and from high to low  
207 are: GA/Fe<sup>2+</sup> > GA/Fe<sup>3+</sup> > GA/Zn<sup>2+</sup> > GA. **There is strong evidence showing that metal ion binding**  
208 **to proteins tends to induce aggregation. The increase in molecular weight of GARTEs may be due**  
209 **to metal ions binding to proteins, inducing partial aggregation of gum arabic fractions. Given that**  
210 **the increase in average molecular weight and the AGP content are relatively modest, the results**  
211 **indicate that GA molecules are still largely present in non-aggregated form in GARTEs.**  
212 **According to relevant literature reports,** Fe<sup>3+</sup>, Fe<sup>2+</sup> and Zn<sup>2+</sup> have a significant effect on the  
213 mechanism of protein aggregation (Bonda, *et al.*, 2011; Sensi, *et al.*, 2009; Töugu, Tiiman, &  
214 Palumaa, 2011; Timasheff, 1998). Multivalent metal ions are especially efficient in this  
215 stabilization by bringing together charged residues on the protein surface (Maclean, Qian, &  
216 Middaugh, 2002). The **likely** changes are illustrated schematically in Fig. 1. In the present system,  
217 **metal ions binding might promote the folding of protein fraction of gum arabic into aggregation-**  
218 **prone conformations and thus accelerate their aggregation** (Lang & Kohn, 1970; Vitos, *et al.*,  
219 1998). Nevertheless, different metal ions have different effects on protein aggregation process.  
220 The results show that the effect of different metal ions of GARTE on protein aggregation process  
221 decreases in the order GA/Fe<sup>2+</sup> > GA/Fe<sup>3+</sup> > GA/Zn<sup>2+</sup>. Jishnu and Umesh (Jishnu & Umesh, 2017)  
222 investigated that metal ions influences on the conformation and aggregation processes of bovine  
223 β-lactoglobulin (β-Ig) at equimolar ratio under thermal condition. Fe<sup>3+</sup> ion causes a more drastic  
224 perturbation of the conformation of native β-Ig than Zn<sup>2+</sup> ion. β-Ig is prone to form irreversible

225 aggregates probably by the metal-complex formation. The  $\beta$ -lg aggregates with  $\text{Zn}^{2+}$  are fibrillar  
226 in nature while the higher molecular aggregates with  $\text{Fe}^{3+}$  ion are of different types. Therefore, the  
227 kinetic growth and the shape of the protein aggregates with different metals solely depend on the  
228 nature of the metal ions, not on the charge of the metal ions.

## 229 3.2 Emulsifying performance of GARTE

### 230 3.2.1 The kinetics of adsorption

231 The GA,  $\text{GA}/\text{Zn}^{2+}$ ,  $\text{GA}/\text{Fe}^{3+}$  and  $\text{GA}/\text{Fe}^{2+}$  solutions were used as the aqueous phase with a  
232 concentration of 0.5% and MCT as the oil phase to determine the dynamic adsorption of GA and  
233 GARTE on the interface of MCT-water. The dynamics of GA and GARTE adsorption at an  
234 MCT-water interface was examined over the time scale ranging from seconds to several hours.  
235 Interfacial tensions measured during the adsorption of different GARTEs onto the MCT-water  
236 interface at 25 °C are shown in Fig. 2. It can be clearly observed that, the interfacial tension  
237 decreases progressively along with the adsorption time, with faster changes at earlier adsorption  
238 period, indicating a spontaneous adsorption of GA and GARTE at the interface. The decrease is  
239 initially steeper before an asymptotically plateauing after the interface is generated. This shape is  
240 characteristic for the interfacial tension evolution of the emulsifier laden oil/water interface. ~~It is~~  
241 ~~attributed to a two stage process: the initial fast diffusion of emulsifier to the interface followed by~~  
242 ~~a slower adsorption delayed by electrostatic and steric hindrance (Felix, Romero, Vermant, &~~  
243 ~~Guerrero, 2016; Noskov, 2014).~~ However, the initial interfacial tension of GARTE is significantly  
244 higher than that of GA, indicating that the adsorption rate of GARTE at the MCT-water interface  
245 has decreased. The time required for reducing interfacial tension by 30% of the initial value at the  
246 MCT-water interface due to the adsorption of GA,  $\text{GA}/\text{Zn}^{2+}$ ,  $\text{GA}/\text{Fe}^{3+}$  and  $\text{GA}/\text{Fe}^{2+}$  and the  
247 equilibrium interfacial tension at 40,000 s at 25°C are shown in Table 3. ~~GA shows more rapid~~  
248 ~~adsorption dynamics than GARTEs and better ability to reduce the equilibrium interfacial tension.~~  
249 It indicates that the adsorption rate of GARTE decreases with enriched  $\text{Zn}^{2+}$ ,  $\text{Fe}^{3+}$  and  $\text{Fe}^{2+}$ . The  
250 interfacial tension of GARTE after the interface adsorption has reached its equilibrium is also  
251 significantly higher than the control GA. The magnitude of interfacial tension  $\gamma$  after adsorption  
252 equilibrium is as follows:  $\gamma (\text{GA}/\text{Fe}^{2+}) > \gamma (\text{GA}/\text{Fe}^{3+}) > \gamma (\text{GA}/\text{Zn}^{2+}) > \gamma (\text{GA})$ . Many factors such

253 as emulsifier size, hydrophobicity, instability, charge, and disulfide bonds are considered in  
254 determining adsorption rate among the different emulsifiers. Beverung *et al.* investigated  
255 adsorption kinetics of different proteins (bovine serum albumin,  $\beta$ -Casein and ovalbumin) at the  
256 oil-water interface by dynamic interfacial tension measurements (Beverung, Radke, & Blanch,  
257 1999). Their results showed that higher molecular weight proteins have a higher interfacial tension  
258 at the initial stage and a slower rate of interfacial tension decrease than smaller molecular weight  
259 proteins. The adsorption rates of GA and GARTE are possibly associated with the molecular  
260 weights of GA, GA/Zn<sup>2+</sup>, GA/Fe<sup>3+</sup> and GA/Fe<sup>2+</sup>, due to the fast adsorption of low molecular  
261 weight species during droplet formation (Gould & Wolf, 2017). As shown in Fig. 1, partial  
262 aggregation of proteins caused by metal ions binding increases the large molecular weight  
263 components (AGP) in GARET and decreases the small molecular weight component (AG and  
264 GP). This might explain the different interfacial adsorption behaviors of GA and GARET, and  
265 further their emulsifying performance to be discussed below.

### 266 3.2.2 Droplet size and distribution

267 The droplet size distributions and volume mean diameters ( $D[4, 3]$ ) of the freshly prepared and  
268 accelerated emulsions stabilized by GA and GARTE were determined and compared for the  
269 evaluation of their emulsifying capacity (Fig. 3 and Fig. 4). The emulsions contain 5.0% GA or  
270 GARTE with 5% MCT as mentioned in experimental section. These emulsions have similar  
271 droplet size distribution at 60°C over a week. The emulsion freshly prepared with GA alone  
272 exhibits a small droplet size ( $d \approx 0.41 \mu\text{m}$ ), which could be related with the relatively high surface  
273 activity of GA at the oil-water interface. The accelerated emulsion shows a little increase in  
274 droplet size ( $d \approx 0.51 \mu\text{m}$ ) with a slight shift of size distribution profiles to the right. When  
275 incorporated with trace elements, the freshly prepared GARTE emulsions show a smaller particle  
276 size ( $p < 0.05$ ) than GA. Noticeably, no significant ( $p > 0.05$ ) changes in particle size for  
277 accelerated emulsion  $D[4, 3]$  are observed during storage time up to 7 days, indicating a high  
278 stabilizing ability of GARTE against coalescence. Visual observation of the emulsions prepared  
279 with GA and GARTE is shown in Fig. 3B. Emulsions prepared with GARTE all exhibit excellent  
280 bulk stability during acceleration. Castellani *et al.* investigated the emulsifying properties and the  
281 adsorption behaviors at the n-hexadecane–water interface of conventional arabic gum and those

282 after thermal maturation (EM1 and EM2) (Castellani, Gaillard, *et al.*, 2010; Castellani, Guibert, *et*  
283 *al.*, 2010). They found that thermal maturation resulted in an increase in average molecular weight  
284 and arabinogalactan protein (AGP) content. It further led to a decrease in interfacial adsorption  
285 kinetics but a more homogenous and stable emulsion. The emulsifying performance of matured  
286 gum seems to be similar with that of GARTE. The improved emulsifying property might be  
287 related to the better interfacial steric stabilizing effect of aggregated GA molecules in GARTE,  
288 which form a thicker interfacial layer and more efficiently prevent emulsion droplets from  
289 coalescence. This resulted in emulsions with smaller droplets and better stability.

### 290 3.2.3 Zeta potential of GA and GARTE emulsion

291 The surface charge of the GA and GARTE stabilized droplets was assessed through measuring  
292 zeta potentials (see Fig. 5 for the results). The data were acquired following the dilution of each  
293 emulsion with water and all GA and GARTE stabilized emulsions show a relatively high negative  
294 zeta potential. A zeta potential of 30 mV is often reported as a critical value below which  
295 emulsions are seen to flocculate (Grumezescu, 2016), requiring the addition of thickening agents  
296 to prevent creaming. Here, while the absolute values of the zeta potential of the GA and GARTE  
297 stabilized emulsions are more than 30 mV, the emulsions show no coalescence or flocculation  
298 over 7 days at 60°C. The zeta potential absolute values of fresh and accelerated emulsions of  
299 GA/Zn<sup>2+</sup> and GA/Fe<sup>2+</sup> were lower than GA emulsions. This might be due to GA/Zn<sup>2+</sup> and  
300 GA/Fe<sup>2+</sup> binding positively charged Zn<sup>2+</sup> and Fe<sup>2+</sup> ions after ion exchange, thereby reducing the  
301 absolute value of zeta potential. Although the zeta potential of GA/Zn<sup>2+</sup> and GA/Fe<sup>2+</sup> is slightly  
302 reduced compared with GA, it is still large enough to provide an effective electrostatic stabilizing  
303 effect (> 45 mV). Additionally, as discussed above, the aggregation in GA/Zn<sup>2+</sup> and GA/Fe<sup>2+</sup>  
304 tends to provide a better interfacial steric stabilizing effect. These together led to a better stability  
305 of emulsions stabilized with GA/Zn<sup>2+</sup> and GA/Fe<sup>2+</sup> (Castellani, Guibert, *et al.*, 2010). In the case  
306 of the GA/Fe<sup>3+</sup> stabilized emulsions, the absolute value of the zeta potential was significantly  
307 higher compared to the other emulsions. The reason for this is unknown at the present stage, and is  
308 possibly due to the fact that the binding affinity of Fe<sup>3+</sup> with GA is weaker than those of Zn<sup>2+</sup> and  
309 Fe<sup>2+</sup> and other divalent cations such as Ca<sup>2+</sup> and Mg<sup>2+</sup>, leading to a larger extent of dissociation  
310 from GA and therefore a higher zeta potential. Nevertheless, long term stability of GARTEs,

311 comparable to GA stabilized emulsions, can also be assumed. These results indicate that the use of  
312 GARTEs as an emulsifier is comparable, if not more efficient, to GA, offering a trace element  
313 source of natural functional polysaccharide for food emulsion formulations.

#### 314 4. Conclusions

315 This research has combined organic and inorganic materials to produce cost-effective trace  
316 element-polysaccharides. It can be validated that GA can be effective carriers for trace elements  
317 for food fortification. The resulting hybrid materials can be utilized to stabilize o/w emulsions  
318 without significant droplet coalescence for a period of at least a week under harsh environment.  
319 The stability in o/w emulsions combined with its low cost demonstrate that the zinc or iron-  
320 polysaccharides are promising novel trace elements fortificants in food products.

321

#### 322 Acknowledgements

323 This work was supported by the state key research and development plan "modern food  
324 processing and food storage and transportation technology and equipment" (No.  
325 2017YFD0400200), National Natural Science Foundation of China (31671811), Hubei  
326 Provincial Youth Natural Science Foundation (No. 2018CFB414), and the grant from  
327 Shanghai Science and Technology Committee (No. 18JC1410801).

328

#### 329 List of Figures

330 **Fig. 1** Schematic of metal ion binding to proteins tends to aggregation of gum arabic.

331 **Fig. 2** Linear plot of adsorption kinetics of GA, GA/Zn<sup>2+</sup>, GA/Fe<sup>3+</sup>, GA/Fe<sup>2+</sup> at the MCT-water  
332 interface at 25°C.

333 **Fig. 3** Particle size distribution (A) and visual observation (B) of fresh and accelerated emulsions  
334 stabilized with GA, GA/Zn<sup>2+</sup>, GA/Fe<sup>3+</sup> and GA/Fe<sup>2+</sup> at 60°C for 7 days.

335 **Fig. 4** Time evolution in  $D[4, 3]$  of GA, GA/Zn<sup>2+</sup>, GA/Fe<sup>3+</sup>, GA/Fe<sup>2+</sup> stabilized emulsions during  
336 storage at 60°C. Error bars represent the standard deviation of at least two independent replicates.

337 **Fig. 5.** Zeta potential of GA, GA/Zn<sup>2+</sup>, GA/Fe<sup>3+</sup>, GA/Fe<sup>2+</sup> stabilized emulsions during storage at  
338 60°C. Error bars represent the standard deviation of at least two independent replicates.

339

340 **List of Tables**341 **Table 1.** Trace elements content of GA, GA/Zn<sup>2+</sup>, GA/Fe<sup>3+</sup>, GA/Fe<sup>2+</sup> samples342 **Table 2.** Molecular parameters of GA, GA/Zn<sup>2+</sup>, GA/Fe<sup>3+</sup>, GA/Fe<sup>2+</sup> samples measured by GPC-

343 MALLS

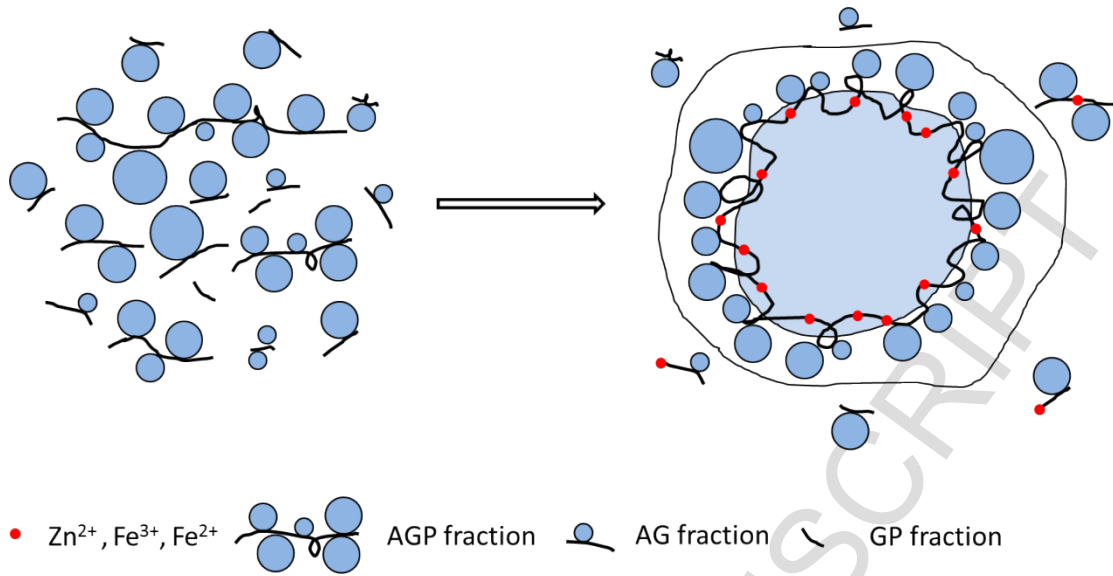
344 **Table 3.** The time (T) required to reduce interfacial tension by 30% of the initial value at the

345 MCT-Water interface and equilibrium interfacial tension at 40000 s at 25°C.

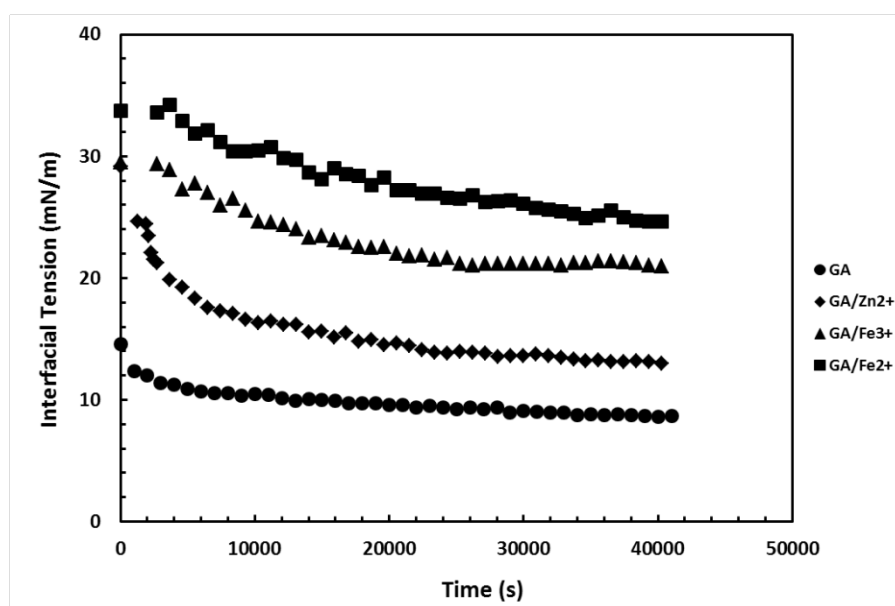
346



347 Fig. 1

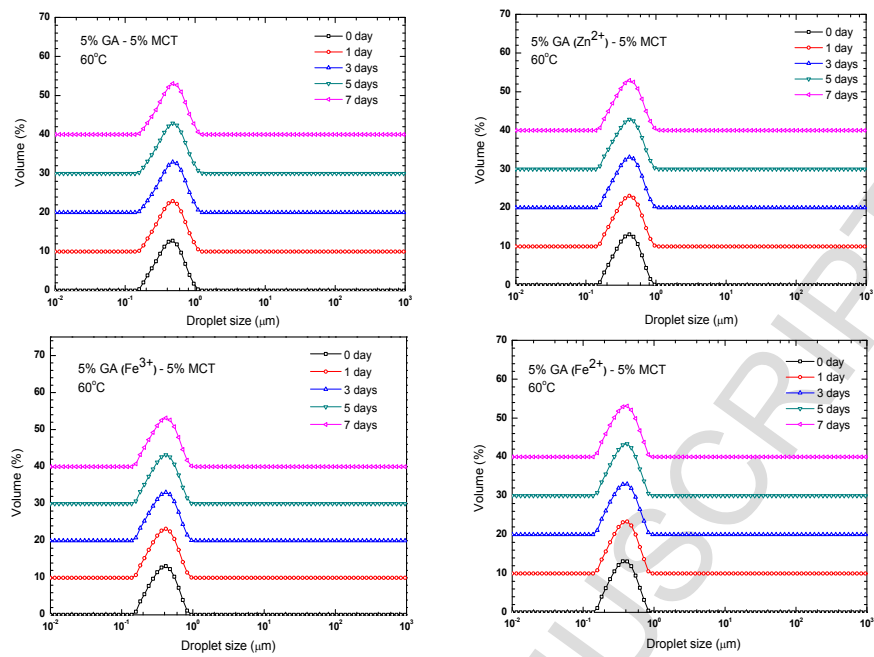


350 Fig. 2



351

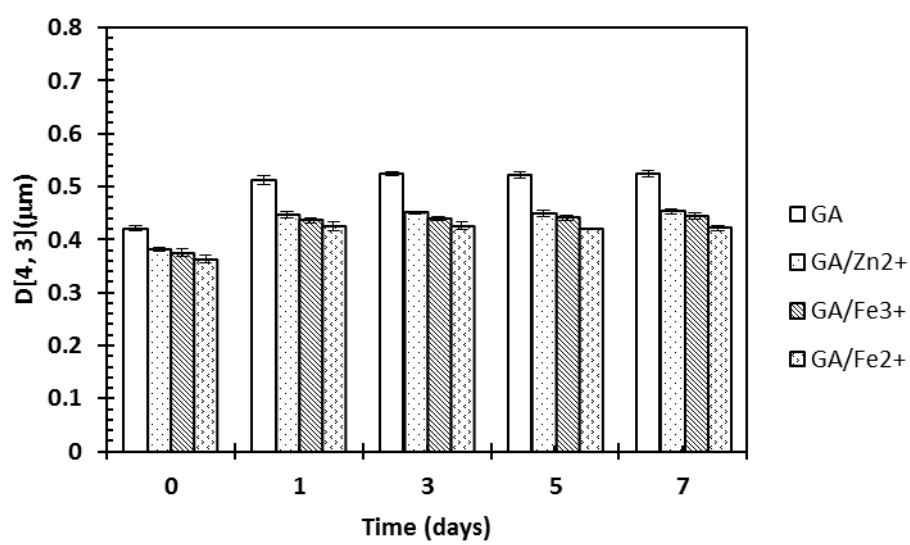
352

353 **Fig. 3****A****B**

354

355

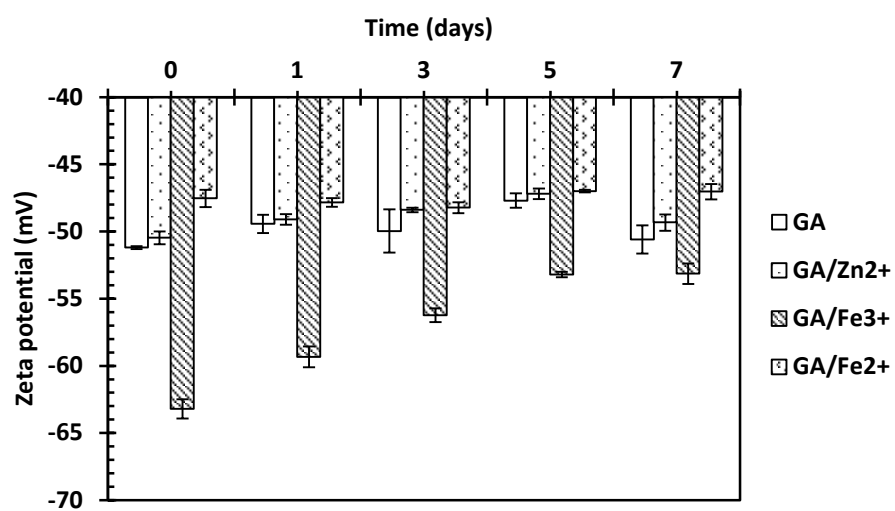
356 Fig. 4



357

358

359 Fig. 5



360

361

362 Table 1.

Sample	Cu (ppm)	Zn (ppm)	Fe (ppm)	K (ppm)	Na (ppm)	Ca (ppm)	Mg (ppm)
GA	<0.01	130.40	5.20	11524.30	8569.90	8287.27	2986.00
GA/Zn <sup>2+</sup>	5.13	3571.40	92.50	2392.40	5380.00	512.82	425.82
GA/Fe <sup>3+</sup>	<0.01	33.99	844.88	3020.20	2399.20	130.72	631.81
GA/Fe <sup>2+</sup>	<0.01	80.79	5705.30	3624.70	3666.50	193.91	232.70

363

364 Table 2.

Sample	Whole	AGP fraction		AG+GP fraction	
	fraction	Percentage	$M_w$	Percentage	$M_w$
	$M_w$ (g/mol)	(wt.%)	(g/mol)	(wt.%)	(g/mol)
GA	$9.43 \times 10^5$	16.86	$3.99 \times 10^6$	83.14	$3.11 \times 10^5$
GA/Zn <sup>2+</sup>	$9.99 \times 10^5$	17.11	$4.23 \times 10^6$	82.89	$3.35 \times 10^5$
GA/Fe <sup>3+</sup>	$1.06 \times 10^6$	17.70	$4.50 \times 10^6$	82.30	$3.32 \times 10^5$
GA/Fe <sup>2+</sup>	$1.37 \times 10^6$	18.51	$5.71 \times 10^6$	81.49	$3.42 \times 10^5$

365

366 Table 3.

Emulsion sample	T (s)	Equilibrium interfacial (mN/m)
GA	4974	8.67
GA/Zn <sup>2+</sup>	7587	13.11
GA/Fe <sup>3+</sup>	8427	20.98
GA/Fe <sup>2+</sup>	38911	24.62

367



368 **References**

- 369 Ali, B. H., Ziada, A., & Blunden, G. (2009). Biological effects of gum arabic: A review of some recent  
370 research. *Food & Chemical Toxicology*, 47(1), 1-8.
- 371 Allen, L., De Benoist, B., Dary, O., & Hurrell, R. (2006). Guidelines on food fortification with  
372 micronutrients. *volume 18*(18), 106-120.
- 373 Beverung, C. J., Radke, C. J., & Blanch, H. W. (1999). Protein adsorption at the oil/water interface:  
374 characterization of adsorption kinetics by dynamic interfacial tension measurements.  
375 *Biophysical Chemistry*, 81(1), 59.
- 376 Bonda, D. J., Lee, H. G., Blair, J. A., Zhu, X., Perry, G., & Smith, M. A. (2011). Role of Metal  
377 Dyshomeostasis in Alzheimer Disease. *Metallomics Integrated Biometal Science*, 3(3), 267.
- 378 Castellani, J. W., Muza, S. R., Chevront, S. N., Sils, I. V., Fulco, C. S., Kenefick, R. W., Beidleman,  
379 B. A., & Sawka, M. N. (2010). Effect of hypohydration and altitude exposure on aerobic  
380 exercise performance and acute mountain sickness. *Journal of Applied Physiology*, 109(6),  
381 1792-1800.
- 382 Castellani, O., Guibert, D., Al-Assaf, S., Axelos, M., Phillips, G. O., & Anton, M. (2010).  
383 Hydrocolloids with emulsifying capacity. Part 1 – Emulsifying properties and interfacial  
384 characteristics of conventional ( *Acacia senegal* (L.) Willd. var. *senegal* ) and matured (*Acacia*  
385 ( *sen* ) SUPER GUM™) *Acacia senegal*. *Food Hydrocolloids*, 24(2–3), 193-199.
- 386 Castellani, O., Al-Assaf, S., Axelos, M., Phillips, G. O., & Anton, M. (2010). Hydrocolloids with  
387 emulsifying capacity. Part 2 – Adsorption properties at the n-hexadecane–Water interface.  
388 *Food Hydrocolloids*, 24(2), 121-130.
- 389 Castellani, O., Gaillard, C., Vié, V., Al-Assaf, S., Axelos, M., Phillips, G. O., & Anton, M. (2010).  
390 Hydrocolloids with emulsifying capacity. Part 3 – Adsorption and structural properties at the  
391 air–water surface. *Food Hydrocolloids*, 24(2–3), 131-141.
- 392 Chakraborty, S., Tewari, S., Sharma, R. K., Narula, S. C., Ghalaut, P. S., & Ghalaut, V. (2014). Impact  
393 of iron deficiency anemia on chronic periodontitis and superoxide dismutase activity: a cross-  
394 sectional study. *Journal of Periodontal & Implant Science*, 44(2), 57-64.
- 395 Chen, J., & Teo, K. C. (2001). Determination of cadmium, copper, lead and zinc in water samples by  
396 flame atomic absorption spectrometry after cloud point extraction. *Analytica Chimica Acta*,  
397 450(1–2), 215-222.
- 398 Dawson, R., Branch-Mays, G., Gonzalez, O. A., & Ebersole, J. L. (2013). Dietary modulation of the  
399 inflammatory cascade. *Periodontol*, 64(1), 161-197.
- 400 Dickinson, E. (2003). Hydrocolloids at interfaces and the influence on the properties of dispersed  
401 systems ☆. *Food Hydrocolloids*, 17(1), 25-39.
- 402 Dupont, C. L., Valas, R. E., Bourne, P. E., & Caetano-Anollés, G. (2010). History of biological metal  
403 utilization inferred through phylogenomic analysis of protein structures. *Proceedings of the*  
404 *National Academy of Sciences of the United States of America*, 107(23), 10567-10572.
- 405 Dupont, C. L., Yang, S., Palenik, B., & Bourne, P. E. (2006). Modern Proteomes Contain Putative  
406 Imprints of Ancient Shifts in Trace Metal Geochemistry. *Proceedings of the National*  
407 *Academy of Sciences of the United States of America*, 103(47), 17822-17827.
- 408 ~~Felix, M., Romero, A., Vermant, J., & Guerrero, A. (2016). Interfacial properties of highly soluble~~  
409 ~~crayfish protein derivatives. *Colloids & Surfaces A Physicochemical & Engineering Aspects*,~~  
410 ~~499, 10–17.~~
- 411 Gaither, L. A., & Eide, D. J. (2001). Eukaryotic zinc transporters and their regulation. *Biometals An*

- 412 *International Journal on the Role of Metal Ions in Biology Biochemistry & Medicine*, 14(3-4),  
413 251-270.
- 414 Gomes, J. F., Rocha, S., Do, C. P. M., Peres, I., Moreno, S., Toca-herrera, J., & Coelho, M. A. (2010).  
415 Lipid/particle assemblies based on maltodextrin-gum arabic core as bio-carriers. *Colloids &*  
416 *Surfaces B Biointerfaces*, 76(2), 449-455.
- 417 Gomes, J. F. P. S., Rocha, S., Pereira, M. D. C., Peres, I., Moreno, S., Toca-Herrera, J., & Coelho, M.  
418 A. N. (2010). Lipid/particle assemblies based on maltodextrin–gum arabic core as bio-carriers.  
419 *Colloids & Surfaces B Biointerfaces*, 76(2), 449-455.
- 420 Gould, J., & Wolf, B. (2017). Interfacial and emulsifying properties of mealworm protein at the  
421 oil/water interface. *Food Hydrocolloids*.
- 422 Grumezescu, A. (2016). *Emulsions*. Elsevier Science.
- 423 Guan, Y., & Zhong, Q. (2014). Gum Arabic and Fe(2+) Synergistically Improve the Heat and Acid  
424 Stability of Norbixin at pH 3.0-5.0. *Journal of Agricultural & Food Chemistry*, 62(52), 12668.
- 425 Hantke, K. (2005). Bacterial zinc uptake and regulators. *Current Opinion in Microbiology*, 8(2), 196-  
426 202.
- 427 Hilty, F. M., Arnold, M., Hilbe, M., Teleki, A., Knijnenburg, J. T. N., Ehrensperger, F., Hurrell, R. F.,  
428 Pratsinis, S. E., Langhans, W., & Zimmermann, M. B. (2010). Iron from nanocompounds  
429 containing iron and zinc is highly bioavailable in rats without tissue accumulation. *Nature*  
430 *Nanotechnology*, 5(5), 374-380.
- 431 Hou, J., Yamada, S., Kajikawa, T., Ozaki, N., Awata, T., Yamaba, S., Fujihara, C., & Murakami, S.  
432 (2014). Iron plays a key role in the cytodifferentiation of human periodontal ligament cells.  
433 *Journal of Periodontal Research*, 49(2), 260-267.
- 434 Jayme, M. L., Dunstan, D. E., & Gee, M. L. (1999). Zeta potentials of gum arabic stabilised oil in  
435 water emulsions. *Food Hydrocolloids*, 13(6), 459-465.
- 436 Jishnu, C., & Umesh, C. H. (2017). Formation of Protein Micro-Spherulites: Thermal Aggregation of  
437 Bovine  $\beta$ -Lactoglobulin with Metal Ions. *International Journal of Scientific & Engineering*  
438 *Research*, 8(3), 23-31.
- 439 Lang, N. D., & Kohn, W. (1970). Theory of Metal Surfaces: Charge Density and Surface Energy.  
440 *Physical Review B Condensed Matter*, 1(1), 4555-4568.
- 441 Li, X., Fang, Y., Al-Assaf, S., Phillips, G. O., Yao, X., Zhang, Y., Zhao, M., Zhang, K., & Jiang, F.  
442 (2012). Complexation of bovine serum albumin and sugar beet pectin: structural transitions  
443 and phase diagram. *Langmuir*, 28(27), 10164-10176.
- 444 Listed, N. (1968). Nutritional anaemias. Report of a WHO scientific group. *World Health Organization*  
445 *Technical Report*, 405, 5.
- 446 Maclean, D. S., Qian, Q., & Middaugh, C. R. (2002). Stabilization of proteins by low molecular weight  
447 multi-ions. *Journal of Pharmaceutical Sciences*, 91(10), 2220-2229.
- 448 Mahendran, T., Williams, P. A., Phillips, G. O., Al-Assaf, S., & Baldwin, T. C. (2008). New insights  
449 into the structural characteristics of the arabinogalactan-protein (AGP) fraction of gum arabic.  
450 *Journal of Agricultural & Food Chemistry*, 56(19), 9269-9276.
- 451 Matzner, Y., Levy, S., Grossowicz, N., Izak, G., & Hershko, C. (1979). Prevalence and causes of  
452 anemia in elderly hospitalized patients. *Gerontology*, 25(2), 113-119.
- 453 Meunier, N., O'Connor, J. M., Maiani, G., Cashman, K. D., Secker, D. L., Ferry, M., Roussel, A. M., &  
454 Coudray, C. (2005). Importance of zinc in the elderly: the ZENITH study. *European Journal*  
455 *of Clinical Nutrition*, 59(2), 1-4.

- 456 Mukhopadhyay, D., & Mohanaruban, K. (2002). Iron deficiency anaemia in older people:  
457 investigation, management and treatment. *Age & Ageing*, *31*(2), 87-91.
- 458 Mulikidjanian, A. Y. (2009). On the origin of life in the zinc world: 1. Photosynthesizing, porous  
459 edifices built of hydrothermally precipitated zinc sulfide as cradles of life on Earth. *Biology*  
460 *Direct*, *4*(1), 1-39.
- 461 Murakami, M., & Hirano, T. (2008). Intracellular zinc homeostasis and zinc signaling. *Cancer Science*,  
462 *99*(8), 1515-1522.
- 463 ~~Noskov, B. A. (2014). Protein conformational transitions at the liquid-gas interface as studied by~~  
464 ~~dilatational surface rheology. *Advances in Colloid & Interface Science*, *206*(2), 222-238.~~
- 465 Oscar, C., Saphwan, A. A., Monique, A., Glyno, P., & Marc, A. (2010). Hydrocolloids with  
466 emulsifying capacity. Part 2-Adsorption properties at the n-hexadecane-Water interface. *Food*  
467 *Hydrocolloids*, *24*(2-3), 121-130.
- 468 Prasad, A. S. (1995). Zinc: an overview. *Nutrition*, *11*(11), 93-99.
- 469 Prentice, A. M. (2005). Macronutrients as sources of food energy. *Public Health Nutrition*, *8*(7a), 932-  
470 939.
- 471 Randall, R. C., Phillips, G. O., & Williams, P. A. (1989). Fractionation and characterization of gum  
472 from Acacia senegal. *Food Hydrocolloids*, *3*(1), 65-75.
- 473 Schifferle, R. E. (2010). Periodontal disease and nutrition: separating the evidence from current fads.  
474 *Periodontol*, *50*(1), 78-89.
- 475 Sensi, S. L., Paoletti, P., Bush, A. I., & Sekler, I. (2009). *Zinc in the physiology and pathology of the*  
476 *CNS*: J. Wiley & Sons ;.
- 477 Swinburn, B. A., & Ravussin, E. (1994). Energy and macronutrient metabolism. *Baillieres Clinical*  
478 *Endocrinology & Metabolism*, *8*(3), 527.
- 479 Tõugu, V., Tiiman, A., & Palumaa, P. (2011). Interactions of Zn(II) and Cu(II) ions with Alzheimer's  
480 amyloid-beta peptide. Metal ion binding, contribution to fibrillization and toxicity.  
481 *Metallomics Integrated Biometal Science*, *3*(3), 250.
- 482 Timasheff, S. N. (1998). Control of protein stability and reactions by weakly interacting cosolvents: the  
483 simplicity of the complicated. *Advances in Protein Chemistry*, *51*(1), 355.
- 484 Tokalioglu, Ş., Kartal, Ş., & Elçi, L. (2000). Determination of heavy metals and their speciation in lake  
485 sediments by flame atomic absorption spectrometry after a four-stage sequential extraction  
486 procedure. *Analytica Chimica Acta*, *413*(1-2), 33-40.
- 487 Toutitou, Y., Proust, J., Carayon, A., Klinger, E., Nakache, J. P., Huard, D., & Sachet, A. (1985).  
488 Plasma ferritin in old age. Influence of biological and pathological factors in a large elderly  
489 population. *Clinica chimica acta; international journal of clinical chemistry*, *149*(1), 37-45.
- 490 Trumbo, P., Yates, A. A., Schlicker, S., & Poos, M. (2001). Dietary reference intakes: vitamin A,  
491 vitamin K, arsenic, boron, chromium, copper, iodine, iron, manganese, molybdenum, nickel,  
492 silicon, vanadium, and zinc. *Journal of the American Dietetic Association*, *101*(3), 294.
- 493 Vitos, L., Ruban, A. V., Skriver, H. L., & Kollár, J. (1998). The surface energy of metals. *Surface*  
494 *Science*, *411*(1-2), 186-202.
- 495 Zhang, Y., & Gladyshev, V. N. (2011). Comparative genomics of trace element dependence in biology.  
496 *Journal of Biological Chemistry*, *286*(27), 23623-23629.

497

498

**Highlights**

- 1) Gum arabic was enriched with trace elements ( $Zn^{2+}$ ,  $Fe^{3+}$ ,  $Fe^{2+}$ ) by ion exchange against  $ZnCl_2$ ,  $FeCl_3$  and  $FeCl_2$ .
- 2) Gum arabic rich in trace elements (GARTE) has good emulsion stability performance with increasing molecular weight and AGP content compared to the control gum arabic.
- 3) Gum arabic rich in trace elements (GARTE) offering a trace element source of natural functional polysaccharide for food emulsion formulations.

ACCEPTED MANUSCRIPT